Anal. Bioanal. Electrochem., Vol. 14, No. 1, 2022, 100-115

Analytical & Bioanalytical Electrochemistry

2022 by CEE
www.abechem.com

Full Paper

Quantitative Monitoring of Cefotaxim Ions by a New Potentiometric Sensor Based on Molecularly Imprinted Polymer

Marzieh Majdi,[1] Farhang Mizani,[2,*] and Ali Mohammad-khah[1,3,*]

[1]*Department of Chemistry, University campus 2, University of Guilan, Rasht, Iran*
[2]*Department of Chemistry, Faculty of Science, Payame Noor University, 19395-4697, Tehran, Iran*
[3]*Department of Chemistry, Faculty of Science, University of Guilan, P.O. BOX: 41938-33697, Rasht, Iran*

*Corresponding Authors, Tel.: +982833375225

E-Mails: Farhangmizani@yahoo.com (F. Mizani); mohammadkhah@guilan.ac.ir (A. Mohammad-khah)

Received: 14 October 2021 / Received in revised form: 27 December 2021
Accepted: 3 January 2022 / Published online: 31 January 2022

Abstract- In the present investigation, a potentiometric sensor using molecularly imprinted polymer (MIP) of Cefotaxime sodium (CS) drug was produced. The MIP was synthesized using CS as a drug, Methacrylic acid as a monomer, and triethylene glycol as a cross-linker. Furthermore, potentiometric sensors were produced by dispersing CS MIP in Ortho-nitro phenyl octal ether and reinforcing it into a PVC matrix (PME) and PVC coated on graphite (CGE). There was a linear electrode response ranging from 3.0×10^{-7} to 1.0×10^{-2} M having 57.9 mV decade^{-1} as slope and a limit of detection of 9.0×10^{-8} M for CGE. The pH-independent region ranged from 4.5 to 9.2, and the flow injection analysis (FIA) system depicted a lifetime exceeding eight weeks. The separate solutions technique was utilized to determine the selectivity coefficients for numerous ions. As indicated by our results, the selectivity coefficients for the entire implemented anions, had a magnitude of $\leq10^{-3}$. The design and assembly of the flow cell were not complicated and extended usage did not overburden the memory. The suggested sensor was successfully used to directly ascertain the levels of both real and synthetic Cefotaxime samples.

Keywords- Coated graphite electrode; Flow injection potentiometry; Molecularly imprinted polymer; Cefotaxime sodium

1. INTRODUCTION

Nowadays, antibiotics play a key role as therapeutic agents against common bacteria and are frequently prescribed during clinical interventions. Therefore, antibiotics have attracted a lot of attention in recent decades but are still plagued with undesirable adverse effects and bacterial resistance. A report was issued by the World Health Organization (WHO) in 2016, about the Global antimicrobial resistance surveillance system (GLASS). It indicated that at least 22 countries confronted a high rate of bacterial resistance among many patients suffering from bacterial infections [1]. Their efficacies have been seriously threatened by drug-resistant bacteria following excessive and arbitrary use of this valuable drug. In addition, antibiotics do not easily degrade in nature and that induces ecological toxicity.

Cefotaxime (CS) sodium as a kind of wide acting and semisynthetic cephalosporin antibiotic has been successfully used to counter a variety of Gram-negative and Gram-positive bacterial infections in humans and animals [2,3]. Most antibiotics can be metabolized and then introduced into water and soil as excipients and the derived products obtained which have led to some inappropriate effects. CS shows noticeable stability in different solutions as their natural degradation rate is reported to be about 20% per 90 days [4]. CS is negligibly released in residual concentrations in the microenvironment. However, it has been observed that the resulting resistant strains and genes cause serious global health issues due to the presence of antibiotics. There are several methods for the determination of Cefotaxime such as chemiluminescence [5], HPLC [6], spectrofluorometry [7], voltammetry [8], and capillary zone electrophoresis [9]. All the above routes show excellent sensitivity and selectivity, but the main problem is that analysis and sample preparation processes are time-consuming and tedious. So a facile method with fewer response times is needed.

During the last decades, the field of sensors has received considerable attention. The ion-selective electrodes in potentiometric sensors play a major role in the detection of CS due to their rapid feedback, straightforward measurement, and easy reproducibility. There are many cases in which potentiometric sensor arrays are used for classifying and analyzing composite samples such as biological probes, clinical, and food samples. The main advantage of this sensor type is that the samples do not need any pre-treatment process to decrease interferences and the sample matrix effect [10,11]. Furthermore, the Potentiometric technique is used for the determination of target ion or molecule because it is considered an easy, fast, and cheap technique. The potentiometric technique provides a field to organize a collection of ion-selective sensors based on molecularly imprinted polymers (MIPs). The attribute of ion-selective electrodes implanted on a templated polymer was primarily reported by Murray et al. [12]. Just two years later, an improvement was reported by Arnold et al. in which the membrane potential between the prepared sample and inner filling solutions did not require the template to be extracted from the membrane [13]. In recent years, MIP sensors have been widely developed but only a few numbers of them were able to use a potentiometric transducer which

included MIP sensors based on radical polymerization with acrylic or vinylic types of monomers [14], amino acid analog monomers [15], Optoelectronic and Electrochemical transducers [16,17]. More importantly, MIPs possess some good qualities that make these receptors especially appropriate for use as the receptors of the ionophore-based polymeric membrane ion-selective electrodes. They are adopted in the selective recognition of organic and biological species based on their stability, easy production, and inexpensiveness [18]. Therefore, MIPs could effectively be utilized to recognize different kinds of pharmaceutical compounds.

In this project, for the first time, we produced a MIP sensor based on Cefotaxime (CS) sodium (Figure 1) and evaluated its potentiometric properties. Specifically, our objective was to design an electrochemical sensor having a polymer template with CS as the selective agent. The designed sensor was successfully utilized to determine the level of CS in pharmaceutical drugs. The results of this study pave the way for further improvement of effective and low-detection-limit sensing systems.

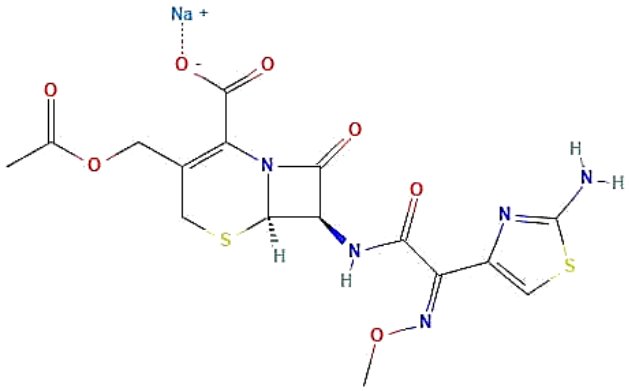

Figure 1. Structure of Cefotaxime sodium (CS)

2. MATERIALS AND METHODS

2.1. Reagents and materials

The reagents used were all obtained commercially and of the best quality without any need for extra purification. The reagents were 2,2´-azobisisobutyronitrile (AIBN), dioctyl phthalate (DOP), Methacrylic acid (MAA), benzyl acetate (BA), ethylene glycol dimethacrylate (EGDMA), O-nitrophenyloctyl ether (O-NPOE), and dibutyl phthalate (DBP). Others included the high molecular weight polyvinyl chloride (PVC) powder, tetrahydrofuran (THF), hexadecyltrimethylammonium bromide (HTAB), and other solvents including inorganic salts. All these were purchased from Merck or Fluka. The potassium or sodium salts of the anions (from Merck or Sigma Aldrich) were of the greatest available purity. During the experiment, double-distilled water was utilized accordingly as a dissolution base. Cefotaxime sodium was gifted by Alborz daru pharmaceutical company (Industrial City, Qazvin, Iran). Cefotaxime

sodium pills were locally procured from a pharmacy. Standard solutions were freshly prepared with double-distilled water.

2.2. MIP synthesis

0.2 mg cefotaxime sodium drug was deposited into a polymerization tube and 35mg acetonitrile/15mg DMSO (or chloroform or methanol) solvent was added to it. Meta acrylic acid monomer (0.6 to 1.8mL) was added to the tube to form a complex between the monomer and the drug. 16mL triethylene glycol was supplemented as a crosslinker followed by an ultrasonic process. Additionally, 0.45mg benzyl peroxide (or azobis or butyl per benzoate) was also incorporated as an initiator proceeded by another ultrasonic process respectively. NIP was prepared exactly like the MIP process, but without the addition of CS drug. 10% acetic acid in methanol was used for washing MIP samples.

2.3. Potentiometric electrode production

For the preparation of potentiometric electrodes (PME), 30mg PVC powder, 60mg O-NPOE plasticizer, 1-5mg HTAB additive, and 10mg MIP were added to THF solvent and mixed with a magnetic stirrer for 30 mins. By evaporating the solvent in a glassy tube containing the material, an electrode was made by compacting the material to a thickness of 0.3mm in the glassy tube. 1×10^{-3} molar CS drug was prepared as the internal solution. Furthermore, Ag/Agcl electrode was put into the glassy tube as the reference electrode. CGE was prepared exactly like PME. The internal solution was not needed for the CGE electrodes.

2.4. Analysis and measurements

All measurements were done in the laboratory using a digital multi-meter Hioki, Model 3256-50 at 25°C. The electrodes were filled with the internal solution and the reference electrode was added to the setup. This collection accompanied by a calomel external reference electrode was utilized to examine the operational state of the MIP electrode. The potential of the electrode was calibrated against the drug. The electrical potential of the electrodes was evaluated employing the silver chloride electrochemical cell:

Ag/AgCl | internal solution, 1.0×10^{-3}M CS | PVC membrane | test solution | Hg–Hg_2Cl_2, KCl (sat'd).

Magnetic stirrer, Delta Model HM-101, ultrasonic equipment, Sa Iran model, and Hg/Hg_2Cl_2 and Ag/AgCl electrodes produced by Azar Electrode Company (Urmia, Iran) were used in this investigation. The pH was determined digitally with the Metrohum pH meter

(Model 827). Furthermore, the microstructure and thermal properties of MIP were analyzed by SEM JEOL-JSM 5310 and DTA/TG, NETZSCH, STA 449C Jupiter, respectively.

3. RESULTS AND DISCUSSIONS

3.1. Optimization of MIP synthesis

In the present investigation, the amount of absorption calculated by the spectrophotometry method was determined as the target function for the optimization of MIP. Fig. 2 shows the calibration curve for converting the amount of absorption to the concentration of cefotaxime sodium drug.

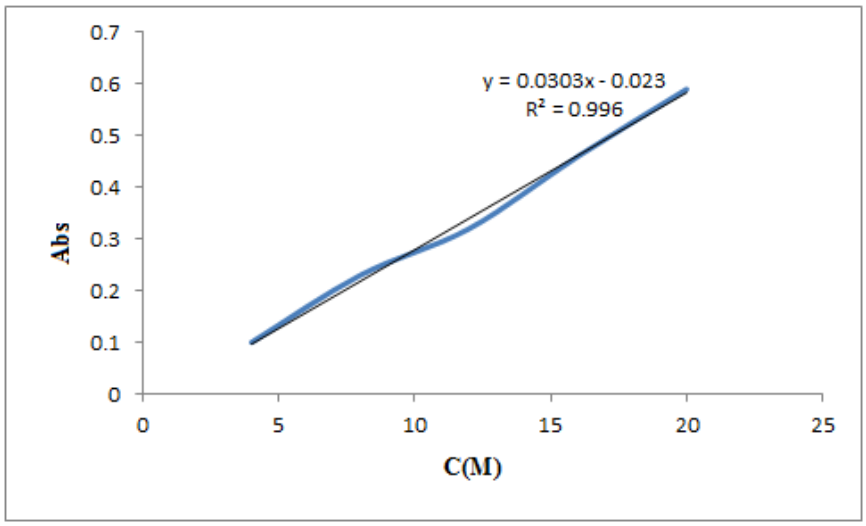

Figure 2. Calibration curve of absorption of cefotaxime sodium drug in various concentrations

The fitted equation of fig.1 is as follows;

$$Y = 0.0303X - 0.023 \quad (1)$$

The correlation coefficient of eq. (1) is 0.996. The distribution coefficient (KD) was used for the comparison of the workability of MIPs. KD is defined by,

$$KD = {}^{Cp}/_{Cs} \quad (2)$$

where C_p is the concentration of drug in polymer and C_s is the concentration of drug in solution. Furthermore, the percentage of drug extraction (Extraction %) by MIPs was determined using the following equation,

$$Extraction\% = \frac{Ci-Cf}{Ci} \quad (3)$$

where, C_i and C_f are the concentrations of the drug before and after extraction from solution, respectively.

To examine the quantity of drug absorbed, the following procedure was executed. Initially, 40mg of MIP was pumped into 15mL of 20ppm solution of drugs. Then the solution was stirred for 1 hour magnetically at a rate of 500rpm. The amount of absorption was calculated by the maximum intensity of absorption from the spectrophotometer spectrum. Using Eq. (1) to (3), the amount of drug extracted using MIP was calculated.

According to previous publications in this field [19-31], several factors were determined as effective parameters for the optimization of MIP which vary at different concentrations. Table 1 shows the controlled factors for the optimization of synthesized CS-MIP.

Table 1. Controlling factors for optimization of CS-MIP synthesis

Controlling factors	Levels		
	1	2	3
Drug/monomer ratio	1:3	1:5	1:7
Initiator	AIBN	Benzoyl peroxide	Butyl per-benzoate
Solvent	Acetonitrile/methanol	Acetonitrile/chloroform	Acetonitrile/DMSO

As illustrated above, three factors changed at three different levels. Therefore, the L9 orthogonal array was utilized for the Taguchi optimization process. Table 2 shows the L9 array designed for the optimization of MIP synthesis.

Table 2. L9 orthogonal array for optimization of MIP synthesis

Number of experiments	Controlling factors		
	Drug/monomer ratio	Initiator	Solvent
1	1:3	AIBN	Acetonitrile/methanol
2	1:3	Benzoyl peroxide	Acetonitrile/chloroform
3	1:3	Butyl per-benzoate	Acetonitrile/DMSO
4	1:5	AIBN	Acetonitrile/DMSO
5	1:5	Benzoyl peroxide	Acetonitrile/methanol
6	1:5	Butyl per-benzoate	Acetonitrile/chloroform
7	1:7	AIBN	Acetonitrile/chloroform
8	1:7	Benzoyl peroxide	Acetonitrile/DMSO
9	1:7	Butyl per-benzoate	Acetonitrile/methanol

Experiments in table 2 were done five times and the amount of absorption was calculated for them. Table 3 shows the amount of absorption for each experiment.

Table 3. The amount of absorption for different experiments

Number of experiments	The amount of absorption (%)					
	1	2	3	4	5	mean
1	75	73	72	74	76	74
2	76	78	80	79	77	78
3	75	74	77	76	78	76
4	81	83	82	83	81	82
5	87	79	82	83	84	83
6	86	85	84	87	84	85
7	83	84	85	82	86	84
8	89	92	93	91	91	91
9	85	86	83	86	88	86

According to Table 3, experiment number 8 had the maximum amount of the mean value of absorption. Hence, its factors and levels were chosen as the optimum condition for CS-MIP synthesis. Table 4 shows the optimum levels of the controlling factors.

Table 4. Optimum levels of controlling factors

Controlling factor	Optimum amount
Drug/monomer ratio	1:7
Initiator	Benzyl per-oxide
Solvent	Acetonitrile/DMSO

Table 5 shows the participation/contribution percentage of various parameters calculated using ANOVA analysis.

Table 5. Participation percentage of parameters for MIP synthesis

Parameter	Percentage
Drug/monomer ratio	58%
Initiator	26%
Solvent	9%
Noise	7%

As demonstrated, the most important parameter was the drug to monomer ratio. Contrarily, the nature or type of solvent had the least amount of participation in results. Therefore, it could

be considered as noise. It is worth noting that the amount of noise is the least factor to be considered for the accurate selection of controlling factors. Fig. 3 shows the SEM micrographs of washed and unwashed CS-MIP.

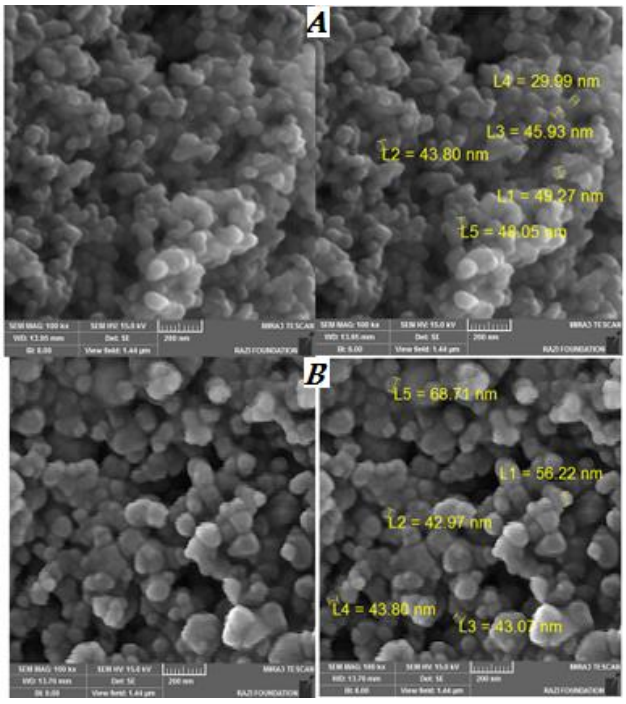

Figure 3. SEM images of (A) unwashed and (B) washed optimum CS MIP

For the examination of the morphology of optimum CS-MIP, SEM analysis was used. Predictably, the morphology of the polymeric particles would be spherical due to the high amount of monomer, and the use of acetonitrile as solvent. The vacancies created by the washing process were obvious in the washed sample. The size of particles was determined to be approximately 50 nm and was semi-spherical. Figure 4 illustrates the TGA curves of NIP and leached and un-leached CS-MIP.

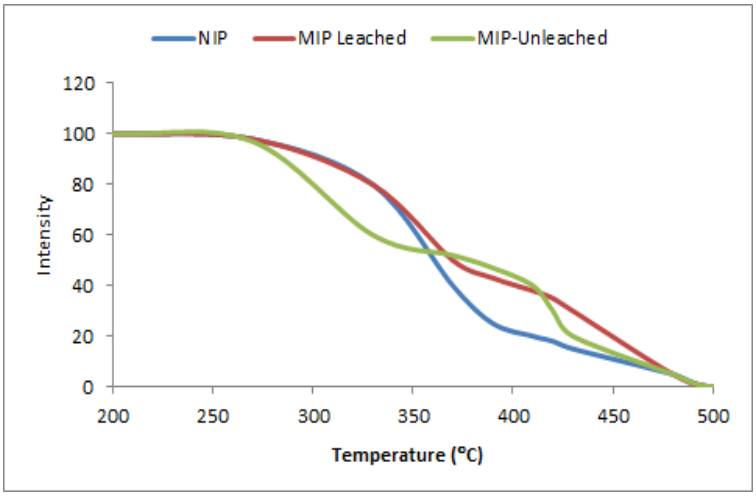

Figure 4. TGA curves of NIP leached and un-leached CS MIP

As illustrated in Figure 4, the first weight reduction occurred at 270°C and it was the same for all three samples. Besides, the intensity of weight reduction was more severe for the un-leached sample. This weight reduction could be attributed to the breakdown of weak chemical bonds. Furthermore, there is another weight reduction for MIP samples at 430°C that could be attributed to the breakdown of bonds between the polymer and the drug. According to fig. 2 and 3, the formation, bonding, and morphology of CS-MIP can easily be visualized.

3.2. Impact of the membrane composition

The sensitive and selective properties of ion-selective electrodes have been established to be remarkably dependent on the quality of the ion carrier, the composition of the membrane, and the solubility of solvent and additives employed [32-36]. As a result, we investigated the effect of these properties on the reaction of the CS sensor (Table 6).

Table 6. Optimization of membrane components for the DSP sensor established by MIP

No.	Membrane composition (%w/w)								Linear range	Slope[a]
	PVC	MIP	AP	BA	DOP	*O*-NPOE	DBP	Additive	[M]	(mV/decade)
1	40	0.0[b]	-	-	-	50	-	3 (HTAB)	----	4.5
2	43	7	-	-	-	50	-	-	$5.0\times10^{-1} - 1.0\times10^{-5}$	-24.3
3	40	10	-	-	-	50	-	-	$3.0\times10^{-1} - 5.0\times10^{-6}$	-35.2
4	37	13	-	-	-	50	-	-	$7.0\times10^{-1} - 5.0\times10^{-6}$	-33.9
5	35	10	-	-	-	55	-	-	$5.0\times10^{-1} - 3.0\times10^{-6}$	-39.1
6	45	10	-	-	-	45	-	-	$4.0\times10^{-1} - 5.0\times10^{-6}$	-37.8
7	35	10	-	-	55	-	-	-	$5.0\times10^{-1} - 3.0\times10^{-5}$	-34.1
8	35	10	-	55	-	-	-	-	$2.0\times10^{-1} - 1.0\times10^{-5}$	-31.1
9	35	10	55	-	-	-	-	-	$3.0\times10^{-1} - 5.0\times10^{-5}$	-25.5
10	35	10	-	-	-	-	55	-	$3.0\times10^{-1} - 1.0\times10^{-5}$	-33.7
11	33	10	-	-	-	55	-	2 (HTAB)	$5.0\times10^{-1} - 1.0\times10^{-6}$	-45.7
12	**31**	**10**	**-**	**-**	**-**	**55**	**-**	**4 (HTAB)**	$\mathbf{1.0\times10^{-6} - 1.0\times10^{-6}}$	**-58.5**
13	29	10	-	-	-	55	-	6 (HTAB)	$1.0\times10^{-1} - 1.0\times10^{-6}$	-54.1

[a] Mean of the slopes measured in triplicates

[b] Membrane composite with 7% MIP

In standard ionophore-based sensors, the reaction time, working concentration range, and slope depend on the ionophore-PVC ratio [78]. On the other hand, the ratio of the PVC-MIP particle is a major determinant in the performance of sensors in ion-selective electrodes with imprinted polymer. This results from the impact of the amount of MIP particles that determine the number of binding sites available for selective rebinding of CS [79]. The results in Table 6

indicate that the membrane with a PVC-MIP ratio weight of 31:10 had the best outcome in terms of performance.

Whereas the lipophilicity and molecular weight of the plasticizer employed in the membrane should be high, its exudation tendency from the polymer matrix and vapor pressure should be small. On the other hand, its ability to dissolve the substrate and membrane additives should be high [77]. Moreover, it should also possess sufficient viscosity and dielectric constant. The composition of a membrane solvent or plasticizer has a great impact on all the electrochemical properties as well as the potentiometric selectivity. This results from its ability to influence the ionic or molecular movement in the membrane, including the membrane dielectric constant. Consequently, we tested different compositions of membranes by altering the quantity and type of plasticizer (Table 6). We used five different plasticizers with varying dielectric constants such as *O*-NPOE, BA, DBP, AP, and DOP to study the impact of the plasticizer composition on CS response. As illustrated in Table 6, *O*-NPOE having the greatest dielectric constant was the most sensitive in terms of response potential.

By forming a congruent and transparent membrane, the *O*-NPOE incorporated membrane demonstrated better compatibility with MIP amid the five different plasticizers utilized. It also produced a greater slope that had a broader range of linear responses. When the plasticizer was excluded, we observed that the MIP-based membranes became fragile and the activity of the sensor could not be verified. It is well established that the addition of cations enhances the EMF response of the anion-selective electrodes. As illustrated in Table 6, the presence of HTAB in the membrane composition (no. 11-13) augments the responsiveness of the sensors. The membrane (no. 12) with a 0.4 optimum percentage ratio of HTAB/MIP revealed a Nernstian response to the concentration of Cefotaxime. Table 6 also shows that the PVC membrane electrode having PVC:O-NPOE:MIP:HTAB percentage ratio of 31:55:10:4, demonstrated the Nernstian behavior of the membrane electrodes across a broad range of concentrations.

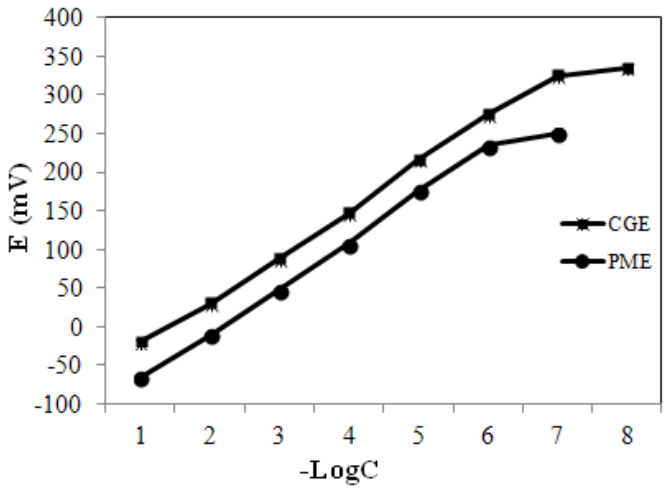

Figure 5. Calibration graphs for the PME and CGE

3.3. Calibration Curve and Detection limit

The basic reactive properties of the prospective sensor were evaluated following IUPAC guidelines [37]. The EMF response of the polymeric membrane (Figure 5) indicates a Nernstian slope of -58.5±0.5 mV per decade over a very wide concentration of Cefotaxime from 1.0×10^{-1}-1.0×10^{-6} M for PME, and a slope of -57.9±0.3 mV per decade over a very wide concentration from 1.0×10^{-2}-3.0×10^{-7} M for PME.

The limit of detection, defined as the concentration of Cefotaxime obtained when extrapolating the linear region of calibration graph to the baseline potential, is 8.0×10^{-7}M and 9.0×10^{-8} M for PME and CGE, respectively.

3.4. pH effect on the electrode response

The influence of the pH of the test solutions (1.0×10^{-3} M of CS^-) on the potential responses of the membrane sensor was tested in the pH range 2.0-11, and the results are shown in Figure 6. As can be seen, the potentials remained constant at the pH range of 4.5-9.5. At higher alkaline media, the potential changed sharply, most probably due to the response of the sensor to both CS^- and hydroxide ions. At a pH lower than 4.5, due to the protonation of CS ions, the potential response of the sensor decreased. In general, MIP-based sensors at pH 6.5 showed the best analytical performance, with the higher slopes, near Nernstian behavior, and lower detection limits with an average slope of approximately 58.5mV/decade. Therefore, a pH of 6-7, was chosen for further CS determination by the proposed sensor.

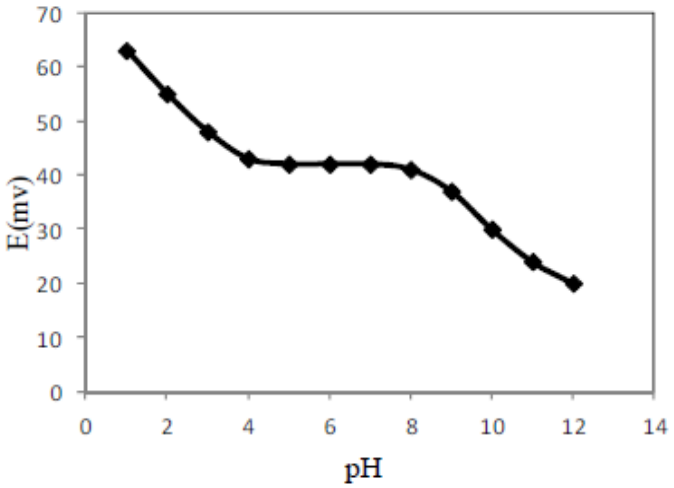

Figure 6. The effect of pH on the potentiometric response of MIP-based CS membrane sensor at concentration 1×10^{-3} M

3.5. Response time of the electrode

The dynamic response time is an important factor for any ion-selective electrode [38-43]. In this study, the response time of the MIP-based membrane ISE is defined as the average time

required for the sensor to reach ±1 mV of the magnitude of the equilibrated potential signal after successful immersion in a series of CS solutions, each having a 10-fold concentration difference and the results are shown in Fig. 7. As it is seen, in whole concentration ranges, the Sensor reached the equilibrium response in a short time (< 25s and < 15s for PME and CGE, respectively).

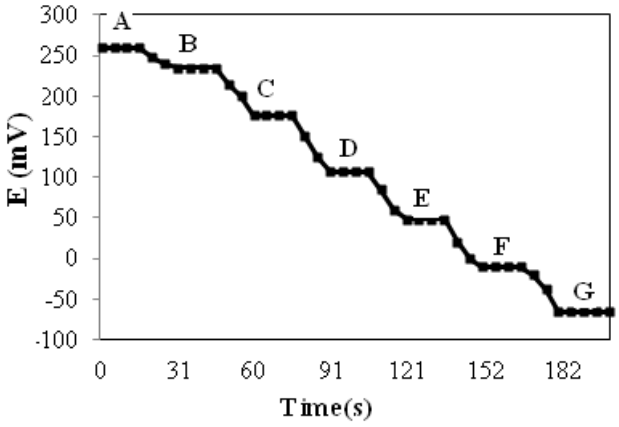

Figure 7. Dynamic response of the MIP-based CS potentiometric sensor for step changes in concentration of CS^- : (A) 1.0×10^{-7}, (B) 1.0×10^{-6}, (C) 1.0×10^{-5}, (D) 1.0×10^{-4}, (E) 1.0×10^{-3}, (F) 1.0×10^{-2} and (G) 1.0×10^{-1} M

3.6. Stability and lifetime

Lifetime studies were based on monitoring the change in the slope of the electrode with time. After 3 months, a very slight decrease in slope (from -58.5 ± 0.4 to -53.5 ± 0.6mV decade-1) of the sensor was observed.

Table 7. Selectivity coefficients of DSP ion-selective electrodes for different anions

Interfering	PME	CGE
$S_2O_3^{2-}$	1.0×10^{-3}	5.0×10^{-4}
IO_3^-	8.5×10^{-4}	4.9×10^{-4}
NO_3^-	7.5×10^{-4}	4.3×10^{-4}
SO_4^{2-}	6.7×10^{-4}	4.0×10^{-4}
Cl^-	5.1×10^{-4}	3.7×10^{-4}
DSP^{2-}	4.3×10^{-4}	3.3×10^{-4}
CO_3^{2-}	4.1×10^{-4}	2.5×10^{-4}
CN^-	3.9×10^{-4}	2.1×10^{-4}
NO_2^-	3.6×10^{-4}	$<10^{-5}$
SCN^-	3.2×10^{-4}	$<10^{-5}$
SO_3^{2-}	$<10^{-5}$	$<10^{-5}$
ClO_4^-	$<10^{-5}$	$<10^{-5}$

3.7. Selectivity coefficients

The average response of an ion-selective electrode to the principal ion compared to other ions in a given solution is the major property of the ion-selective electrode [44,45]. This property is expressed in terms of potentiometric selectivity coefficients. The potentiometric selectivity coefficients (Kpot), describing the preference by the membrane for an interfering ion (An^-) relative to CS^-, were determined by the matched potential method [46]. The results of the selectivity coefficient data with different compositions are given in Table 7.

From the data in Table 7, it is obvious that the selectivity coefficients are in the order of 1.0×10^{-3} or smaller and 5.0×10^{-4} or smaller for PME and CGE respectively. It indicates that these anions have negligible disturbance on the functioning of the CS^- ion-selective electrode.

3.8. Determination of DSP in pharmaceutical formulations

The potentiometric CS membrane sensors can be used for routine analysis and quality control/quality assurance during the manufacture of CS. Potentiometric determination of CS in drug formulations under the static mode of operation was carried out using both direct potentiometry and the standard addition (spiking technique).

Table 8. Determination of DSP in some pharmaceutical preparations using MIP based membrane sensor

Recovery found * (%)				
Sample	Labeled, mg tablet-1	Direct potentiometry	Standard addition	Spectrophotometry
1[a]	100	97.9±0.9	98.8±0.7	99.1±0.8
2[b]	100	98.6±0.8	96.9±0	98.9±0.9

[a] Januvia® tablet (Merck Sharp and Dohme Co., Pavia, Italy)
[b] Janumet® tablet (Merck Sharp and Dohme Co., Cairo, Egypt)

With the direct potentiometric technique, the recoveries were 97.9±0.9 and 98.6±0.8%. The standard addition method showed results with recoveries of 98.8±0.7 and 96.9±0.7% (Table 7). These data were compared with results obtained by the spectrophotometric method [47]. An F-test showed no significant difference at the 95% confidence limit between the means and variances of the results. The calculated F-values (n=10) of the results obtained by the present sensor and different potentiometric techniques (Table 7) for drug tablets were less than 2.5, compared with the theoretically tabulated value (F=3.18).

4. CONCLUSION

In this study, a potentiometric sensor based on molecularly imprinted polymer (MIP) was developed for the determination of Cefotaxime sodium (CS) pharmaceutical compounds. The MIP was synthesized using CS as a template molecule, methacrylic acid as a monomer, and triethylene glycol as a cross-linker. The proposed electrochemical PVC membrane graphite-coated sensor was worked well in a flow injection analysis (FIA) system with a linear of 3.0×10^{-7} to 1.0×10^{-2} M with 57.9 mV decade^{-1} Nernstian slope. As indicated by our results, the selectivity coefficients for the entire implemented anions, had a magnitude of $\leq10^{-3}$. The design and assembly of the flow cell were not complicated and extended usage did not overburden the memory. The sensor was finally used to directly ascertain Cefotaxime in some real samples.

Acknowledgment

We would like to thank Payame Noor University and the University of Guilan for their financial support.

REFERENCES

[1] [Online] available at: World Health Organization, Global antimicrobial resistance surveillance system (GLASS) report Early implementation 2016-2017, https://www.who.int/glass/ resources/publications/early-implementation-report/en/, 2018

[2] H. Zhang, J. Wang, A. Y. Chen, and Q. Nie, J. Chem. Eng. Data 51 (2006) 2239.

[3] R. Gothwal, and T. Shashidhar, Clean-Soil Air Water 43 (2015) 479.

[4] N. F. F. Moreira, J. M. Sousa, G. Macedo, A. R. Ribeiro, L. Barreiros, M. Pedrosa, J. L. Faria, M. F. R. Pereira, S. Castrosilva, and M. A. Segundo, Water Res. 94 (2016) 10.

[5] J. X. Du, and H. Li, Appl. Spectrosc. 64 (2010) 1154.

[6] B. Arabsorkhi, and H. Sereshti, Microchem. J. 140 (2018) 140.

[7] M. A. Omar, O. H. Abdelmageed, and T. Z. Attia, Talanta 77 (2009) 1394.

[8] M. Khan, M. Daizy, C. Tarafder, and X. Liu, Scientific Reports 9 (2019) 1.

[9] R. Wang, Z. P. Jia, J. J. Fan, M. Jun, X. Hua, Q. Zhang, and J. Wang, Pharmazie 64 (2009) 156.

[10] S. Lee, S. Franklin, F. A. Hassani, T. Yokota, M. O. G. Nayeem, Y. Wang, R. Leib, G. Cheng, D. W. Franklin, and T. Someya, Science 370 (2020) 966.

[11] J. F. Masson, ACS Publications 5 (2020) 3290.

[12] G. M. Murray, A. L. Jenkins, A. Bzhelyonsky, and O. M. Uy, J. Hopkins APL Tech. D 18 (1997) 465.

[13] B. R. Arnold, A. C. Euler, and A. L. Jenkins, O. M. Uy, and G. M. Murray, J. Hopkins APL Tech. D 20 (1999) 190.

[14] M. C. Blanco-Lopez, M. J. Lobo-Castanon, A. J. Miranda-Ordieres, and P. Tunon-Blanco, Trends Anal. Chem. 23 (2004) 36.
[15] C. Philip, and K. Devaky, Molecular Catalysis 436 (2017) 276.
[16] J. R. Askim, M. Mahmoudi, and K. S. Suslick, Chem. Soc. Rev. 42 (2013) 8649.
[17] O. S. Ahmad, T. S. Bedwell, C. Esen, A. Garcia-Cruz, and S. A. Piletsky, Trends in Biotechnology 37 (2019) 294.
[18] P. J. Li, R. N. Liang, X. F. Yang, and W. Qin, Mater. Lett. 225 (2018) 138.
[19] H. S. M. Abd-Rabboh, and A. H. Kamel, Electroanalysis 24 (2012) 1409.
[20] R. Liang, L. Kou, Z. Chen, and W. Qin, Sens. Actuators B 188 (2013) 972.
[21] A. H. Kamel, F. T. C. Moreira, A. A. Almeida, and M. F. G. Sales, Electroanalysis 20 (2008) 194.
[22] A. H. Kamel, and F. M. Al Romian, Int. J. Chem. Mat. Sci. 1 (2013) 001.
[23] A. H. Kamel, F. T. C. Moreira, T. I. Silva, and M. G. F. Sales Int. J. Electrochem. (2011) Article ID 643683.
[24] L. J. Kou, R. N. Liang, X. W. Wang, Y. Chen, and W. Qin, Anal. Bioanal. Chem. 405 (2013) 4931.
[25] A. H. Kamel, X. Jiang, P. Li, and R. Liang, Anal. Methods 10 (2018) 3890.
[26] A. H. Kamel, T. Y. Sorora, and F. M. Al Romian, Anal. Meth. 4 (2012) 3007.
[27] A. H. Kamel, F. A. Al Hamid, T. Y. Soror, H. R. Galal, and F. A. El Gendy, Eur. Chem. Bull. 5 (2016) 266.
[28] A. H. Kamel, H. R. Galal, and N. S. Awwad, Anal. Meth. 10 (2018) 5406.
[29] A. H. Kamel, and A. M. E. Hassan, Int. J. Electrochem. Sci. 11 (2016) 8938.
[30] A. M. El-Kosasy, A. H. Kamel, L. A. Hussin, M. F. Ayad, and N. V. Fares, Food Chem. 250 (2018) 250.
[31] A. Merkoci, and S. Alegret, TrAC, Trends Anal. Chem. 21 (2002) 717.
[32] F. Mizani, M. R. Ganjali, F. Faridbod, and S. Esmaeilnia, Int. J. Electrochem. Sci. 8 (2013) 10473.
[33] F. Mizani, and F. Rajabi, Anal. Bioanal. Electrochem. 6 (2014) 206.
[34] F. Mizani, A. Shockravi, M. Taghdiri, S. Bavili Tabrizi, F. Azmoodeh, K. Alizadeh, and M. Shamsipur, J. Incl. Phenom. Macrocycle Chem. 79 (2014) 83.
[35] F. Mizani M. Shamsipur, M. R. Yaftian, and D. Matt, Anal. Sci. 29 (2013) 361.
[36] M. Shamsipur, F. Mizani, M. F. Mousavi, N. Alizadeh, K. Alizadeh, H. Eshghi, and H. Karami, Anal. Chim. Acta 589 (2007) 22.
[37] IUPAC Analytical Chemistry Division, Commission on Analytical Nomenclature Pure. Appl. Chem. 48 (1976) 127.
[38] M. R. Ganjali, M. R. Pourjavid, M. Rezapour, and S. Haghgoo, Sens. Actuators B 89 (2003) 21.

[39] M. R. Ganjali, R. Kiani-Anbouhi, M. Shamsipur, T. Poursaberi, M. Salavati-Niasari, Z. Talebpour and M. Emami, Electroanalysis 16 (2004) 1002.
[40] H. A. Zamani, F. Malekzadegan and M. R. Ganjali, Anal. Chim. Acta 555 (2006) 336.
[41] M. R. Ganjali, S. Rasoolipour, M. Rezapour, P. Norouzi, A. Tajarodi and Y. Hanifehpour, Electroanalysis 17 (2005) 1534.
[42] H. A. Zamani, J. Abedini-Torghabeh and M. R. Ganjali, Electroanalysis 18 (2006) 888.
[43] M. R. Ganjali, P. Norouzi, F. Faridbod, S. Riahi, J. Ravanshad, J. Tashkhourian, M. Salavati-Niasari and M. Javaheri, IEEE Sens. J. 7 (2007) 544.
[44] H. A. Zamani, M. R. Ganjali and M. Adib, Sens. Actuators B 120 (2007) 545.
[45] M. R. Ganjali, P. Norouzi, F. S. Mirnaghi, S. Riahi and F. Faridbod, IEEE Sens. J. 7 (2007) 1138.
[46] Y. Umezawa, K. Umezawa, and H. Sato, Pure. Appl. Chem. 67 (1995) 507.
[47] K. Prakash, K. Sireesha, and A. Shantha Kumar, Int. J. Pharm. Pharm. Sci. 4 (2012) 505.